

# Projected Wavefunctions and High Temperature Superconductivity

Arun Paramekanti, Mohit Randeria and Nandini Trivedi

Department of Theoretical Physics, Tata Institute of Fundamental Research, Mumbai 400005, India

We study the Hubbard model with parameters relevant to the cuprates, using variational Monte Carlo with projected  $d$ -wave states. For doping  $0 < x \lesssim 0.35$  we obtain a superconductor whose order parameter tracks the observed nonmonotonic  $T_c(x)$ . The variational parameter  $\Delta_{\text{var}}(x)$  scales with the  $(\pi, 0)$  “hump” and  $T^*$  seen in photoemission. Projection leads to incoherence in the spectral function and from the *singular* behavior of its moments we obtain the nodal quasiparticle weight  $Z \sim x$  though the Fermi velocity remains finite as  $x \rightarrow 0$ . The Drude weight  $D_{\text{low}}$  and superfluid density are consistent with experiments and  $D_{\text{low}} \propto x$ .

PACS numbers: 74.20.-z, 74.20.Fg, 74.25.-q, 74.72.-h

(December 2, 2024)

Strong correlations are essential to understand  $d$ -wave high temperature superconductivity in doped Mott insulators [1]. The no-double occupancy constraint arising from strong correlations has been treated within two complementary approaches. The gauge theory approach [2] is valid at all temperatures, but it is necessary to include the effects of strong gauge fluctuations. Alternatively, the constraint can be implemented exactly at  $T = 0$  using the variational Monte Carlo (VMC) method. Previous variational studies [3,4] have focussed primarily on the energetics of competing states.

In this paper, we revisit projected wavefunctions of the form proposed by Anderson in 1987 [1]. We compute physically interesting correlations using VMC and show that projection leads to loss of coherence. We obtain information about low energy excitations from the singular behavior of moments of the occupied spectral function. Surprisingly, our results for various observables are in semi-quantitative agreement with experiments on the cuprates. We also make qualitative predictions for the doping ( $x$ ) dependence of correlation functions in projected states (for  $x \ll 1$ ) from general arguments which are largely independent of the detailed form of the wavefunction and the Hamiltonian.

We use the Hubbard Hamiltonian  $\mathcal{H} = \mathcal{K} + \mathcal{H}_{\text{int}}$ . The kinetic energy  $\mathcal{K} = \sum_{\mathbf{k}, \sigma} \epsilon(\mathbf{k}) c_{\mathbf{k}\sigma}^\dagger c_{\mathbf{k}\sigma}$  with  $\epsilon(\mathbf{k}) = -2t(\cos k_x + \cos k_y) + 4t' \cos k_x \cos k_y$  the dispersion on a square lattice with nearest ( $t$ ) and next-near ( $t'$ ) hopping. The on-site repulsion is  $\mathcal{H}_{\text{int}} = U \sum_{\mathbf{r}} n_{\uparrow}(\mathbf{r}) n_{\downarrow}(\mathbf{r})$  with  $n_{\sigma}(\mathbf{r}) = c_{\sigma}^\dagger(\mathbf{r}) c_{\sigma}(\mathbf{r})$ . We work in the strongly correlated regime where  $J = 4t^2/U$ ,  $t' \lesssim t \ll U$  near half filling:  $n = 1 - x$  with the hole doping  $x \ll 1$ . To make comparison with the cuprates, we choose  $t' = t/4$ , with  $t = 300\text{meV}$  and  $U = 12t$  corresponding to  $J = 100\text{meV}$ .

We describe the ground state by the wavefunction

$$|\Psi_0\rangle = \exp(iS)\mathcal{P}|\Psi_{\text{BCS}}\rangle. \quad (1)$$

Here  $|\Psi_{\text{BCS}}\rangle = \left(\sum_{\mathbf{k}} \varphi(\mathbf{k}) c_{\mathbf{k}\uparrow}^\dagger c_{-\mathbf{k}\downarrow}^\dagger\right)^{N/2} |0\rangle$  is the  $N$ -electron  $d$ -wave BCS wave function with  $\varphi(\mathbf{k}) = v_{\mathbf{k}}/u_{\mathbf{k}} = \Delta_{\mathbf{k}}/[\xi_{\mathbf{k}} + \sqrt{\xi_{\mathbf{k}}^2 + \Delta_{\mathbf{k}}^2}]$ . The two variational parameters

$\mu_{\text{var}}$  and  $\Delta_{\text{var}}$  determine  $\varphi(\mathbf{k})$  through  $\xi_{\mathbf{k}} = \epsilon(\mathbf{k}) - \mu_{\text{var}}$  and  $\Delta_{\mathbf{k}} = \Delta_{\text{var}}(\cos k_x - \cos k_y)/2$ . The projector  $\mathcal{P} = \prod_{\mathbf{r}} (1 - n_{\uparrow}(\mathbf{r})n_{\downarrow}(\mathbf{r}))$  in Eq. (1) eliminates all configurations with double occupancy, as appropriate for  $U \rightarrow \infty$ . Finally the unitary transformation  $\exp(iS)$  includes the effects of double occupancy perturbatively in  $t/U$  [5].

Using standard VMC techniques [6] we compute various equal-time correlators in the state  $|\Psi_0\rangle$ . The two variational parameters are determined by minimizing  $\langle\Psi_0|\mathcal{H}|\Psi_0\rangle/\langle\Psi_0|\Psi_0\rangle$  for various values of  $x$ . The doping dependence of the resulting  $\Delta_{\text{var}}(x)$  is shown in Fig. 1(a). Varying input parameters in  $\mathcal{H}$  we find that  $J = 4t^2/U$  sets the scale for  $\Delta_{\text{var}}$ . We show below that  $\Delta_{\text{var}}$  is *not* proportional to the SC order parameter, in contrast to BCS theory, and also argue that it is *not* equal to the spectral gap. On the other hand, we find that the optimal value of  $\mu_{\text{var}}(x)$  is identical with  $\mu_0(x)$ , which is the chemical potential of *noninteracting* electrons described by  $\mathcal{K}$ . We note, however, that  $\mu_{\text{var}}$  is quite different [7] from the chemical potential  $\mu = \partial\langle\mathcal{H}\rangle/\partial N$ , where  $\langle\cdots\rangle$  denotes the expectation value in the optimal, normalized ground state.

**Phase Diagram:** We now show that the wavefunction (1) is able to describe three phases: an RVB insulator, a  $d$ -wave SC and a Fermi liquid metal. To establish the  $T = 0$  phase diagram as a function of  $x$  we first study off-diagonal long range order using  $F_{\alpha,\beta}(\mathbf{r} - \mathbf{r}') = \langle c_{\uparrow}^\dagger(\mathbf{r}) c_{\downarrow}^\dagger(\mathbf{r} + \hat{\alpha}) c_{\downarrow}(\mathbf{r}') c_{\uparrow}(\mathbf{r}' + \hat{\beta}) \rangle$ , where  $\hat{\alpha}$  and  $\hat{\beta}$  can be  $\hat{x}$  or  $\hat{y}$ . We find that  $F_{\alpha,\beta} \rightarrow \pm\Phi^2$  for large  $|\mathbf{r} - \mathbf{r}'|$ , with  $+$  ( $-$ ) sign obtained for  $\hat{\alpha}$  parallel (perpendicular) to  $\hat{\beta}$ , indicating  $d$ -wave SC. As seen from Fig. 1(b) the order parameter  $\Phi$  is *not* proportional to  $\Delta_{\text{var}}$ , and has a rather different  $x$ -dependence: even though  $\Delta_{\text{var}} \neq 0$ ,  $\Phi$  vanishing linearly in  $x$  as  $x \rightarrow 0$ , as first noted in Ref. [3](b). We argue [8] that  $\Phi \sim x$  is a general property of projected SC wavefunctions. The local fixed number constraint imposed by  $\mathcal{P}$  at  $x = 0$  leads to large quantum phase fluctuations that destroy SC order. The non-SC state at half-filling ( $x = 0$ ) is an insulator since it has a vanishing Drude weight, as shown below. The system is a SC in the doping range  $0 < x < x_c \simeq 0.35$  with  $\Phi \neq 0$ .

For  $x > x_c$ ,  $\Phi = 0$  and the wavefunction  $\Psi_0$  for  $\Delta_{\text{var}} = 0$  describes a normal Fermi liquid. In the remainder of this paper we will study  $0 \leq x \leq x_c$ .

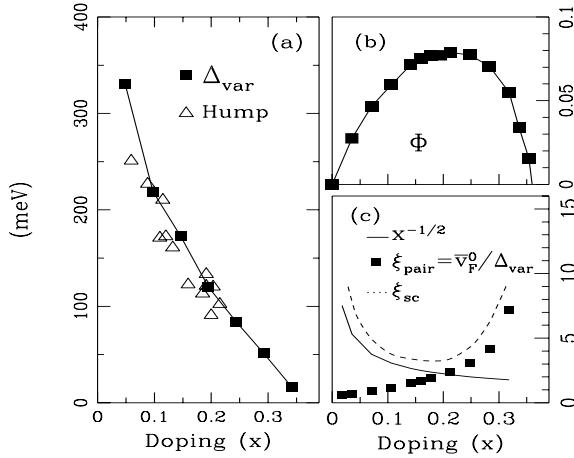


FIG. 1. (a): The variational parameter  $\Delta_{\text{var}}$  (filled squares) and the  $(\pi, 0)$  hump scale (open triangles) in ARPES [9] versus doping. (b): Doping dependence of the  $d$ -wave SC order parameter  $\Phi$ . Solid lines in (a) and (b) are guides to the eye. (c): The coherence length  $\xi_{\text{sc}} \geq \max(\xi_{\text{pair}}, 1/\sqrt{x})$ .

**Coherence Lengths:** We must carefully distinguish between various definitions of ‘coherence lengths’, which differ by factors of order unity in BCS theory, but correspond to very different quantities in the strongly correlated SC studied here. The internal pair wavefunction  $\varphi(\mathbf{k})$  defines a pair-size  $\xi_{\text{pair}} \sim \bar{v}_F^0 / \Delta_{\text{var}}$ , where  $\bar{v}_F^0$  is the Fermi surface averaged, bare (noninteracting) Fermi velocity. The act of projection in (1) does not affect the pair-size much, and  $\xi_{\text{pair}}$  remains finite down to  $x = 0$ , where it defines the range of singlet bonds in the resonating valence bond (RVB) insulator [1].

A second important length scale is the inter-hole spacing  $1/\sqrt{x}$ . SC correlations can exist only on longer scales; at shorter distances there are no holes (vacancies) and the system effectively looks like the  $x = 0$  insulator. Thus the superconducting coherence length  $\xi_{\text{sc}}$  must necessarily satisfy  $\xi_{\text{sc}} \geq \max(\xi_{\text{pair}}, 1/\sqrt{x})$ . This implies that  $\xi_{\text{sc}}$  must diverge both in the insulating limit  $x \rightarrow 0$  (see also Refs. [2]) and the metallic limit  $x \rightarrow x_c^-$ , but is small at optimality; see Fig. 1(c). This non-monotonic behavior of  $\xi_{\text{sc}}(x)$  should be checked experimentally.

**Momentum Distribution:** From gray-scale plots like Fig. 2 we see considerable structure in the momentum distribution  $n(\mathbf{k})$  over the entire range  $0 \leq x \leq x_c$ . One cannot define a Fermi surface (FS) since the system is a SC (or an insulator). Nevertheless, the  $\mathbf{k}$ -space loci (i) on which  $n(\mathbf{k}) = 1/2$  and (ii) on which  $|\nabla_{\mathbf{k}} n(\mathbf{k})|$  is maximum both coincide with the *noninteracting* FS’s within our resolution. Both are large hole-like barrels centered about  $(\pi, \pi)$ , with no change in topology as a function of  $x$ , consistent with angle resolved photoemission spectroscopy (ARPES) [10] on BSCCO ( $\text{Bi}_2\text{Sr}_2\text{CaCu}_2\text{O}_{8+\delta}$ )

and related insulating materials.

We next exploit the fact that moments of dynamical correlations can be expressed as equal-time correlators calculable in our formalism. Specifically, we look at  $M_\ell(\mathbf{k}) = \int_{-\infty}^{\infty} d\omega \omega^\ell f(\omega) A(\mathbf{k}, \omega)$ , where  $A(\mathbf{k}, \omega)$  is the one-particle spectral function and, at  $T = 0$ ,  $f(\omega) = \Theta(-\omega)$ . We calculate  $M_0(\mathbf{k}) = n(\mathbf{k})$  and the first moment [11]  $M_1(\mathbf{k}) = \langle c_{\mathbf{k}\sigma}^\dagger [\mathcal{H}, c_{\mathbf{k}\sigma}] \rangle$  to obtain important information about the spectral function.

**Nodal Quasiparticles:** Fig. 2(c) shows that along  $(0, 0)$  to  $(\pi, \pi)$   $n(\mathbf{k})$  has a jump discontinuity. This implies the existence of gapless quasiparticles (QPs) as observed by ARPES [12]. The spectral function along the diagonal thus has the low energy form:  $A(\mathbf{k}, \omega) = Z\delta(\omega - \tilde{\xi}_k) + A_{\text{inc}}$ , where  $\tilde{\xi}_k = v_F(k - k_F)$  is the QP dispersion and  $A_{\text{inc}}$  the smooth incoherent part. We estimate the nodal  $k_F(x)$  from the location of the discontinuity and the QP weight  $Z$  from its magnitude. While  $k_F(x)$  has weak doping dependence,  $Z(x)$  is shown in Fig. 2(d), with  $Z \sim x$  as the insulator is approached [13].

Projection leads to a suppression of  $Z$  from unity with the incoherent weight  $(1 - Z)$  spread out to high energies. We infer large incoherent linewidths as follows. (a) At the ‘band bottom’  $n(\mathbf{k} = (0, 0)) \simeq 0.85$  (for  $x = 0.18$ ) implying that 15% of the spectral weight must have spilled over to  $\omega > 0$ . (b) Even at  $k_F$ , the first moment  $M_1$  lies significantly below  $\omega = 0$  (defined by the chemical potential  $\mu = \partial\langle\mathcal{H}\rangle/\partial N$ ); see Fig. 3(a).

The moments are dominated by the high energy incoherent part of  $A(\mathbf{k}, \omega)$ , but their *singular behavior is determined by the gapless coherent* QPs. Specifically, along the zone diagonal  $M_1(\mathbf{k}) = Z\tilde{\xi}_k\Theta(-\tilde{\xi}_k) + \text{smooth part}$ . Thus its slope  $dM_1(\mathbf{k})/dk$  has a discontinuity of  $Zv_F$  at  $k_F$ , as seen in Fig. 3(a), and may be used to estimate [14] the nodal Fermi velocity  $v_F$ . As seen from Fig. 3(b),  $v_F(x)$  is reduced from its bare value  $v_F^0$  and is weakly doping dependent, consistent with the ARPES estimate [12] of  $v_F \approx 1.5\text{eV}\cdot\text{\AA}$  in BSCCO.

As  $x \rightarrow 0$ ,  $Z = [1 - \partial\Sigma'/\partial\omega]^{-1} \sim x$ , while  $v_F(x)/v_F^0 = Z[1 + (v_F^0)^{-1}\partial\Sigma'/\partial k]$  is weakly  $x$ -dependent. This implies a  $1/x$  divergence in the  $\mathbf{k}$ -dependence of the self energy  $\Sigma$  on the zone diagonal, which could be tested by ARPES.

**Moments Along  $(\pi, 0) \rightarrow (\pi, \pi)$ :** The moments  $n(\mathbf{k})$  and  $M_1(\mathbf{k})$  near  $\mathbf{k} = (\pi, 0)$  are not sufficient to estimate the SC gap, however they give insight into the nature of the spectral function. As seen from Fig. 4(a)  $n(\mathbf{k})$  is much broader than that for the unprojected  $|\Psi_{\text{BCS}}\rangle$ . For  $\mathbf{k}$ ’s near  $(\pi, \pi)$ , which correspond to high energy, unoccupied ( $\omega > 0$ ) states in  $|\Psi_{\text{BCS}}\rangle$  we see a significant build up of spectral weight transferred from  $\omega < 0$ . Correspondingly, we see loss of spectral weight near  $(\pi, 0)$ . We thus infer large incoherent linewidths at all  $\mathbf{k}$ ’s, directly seen from the large increase in  $|M_1(\mathbf{k})|$  (in Fig. 4(b)) relative to the BCS result.

The transfer of weight over large energies inferred above suggests that projection pushes spectral weight to  $|\omega| < \Delta_{\text{var}}$ , the gap in unprojected BCS theory. We thus

expect that the true spectral gap  $E_{\text{gap}} < \Delta_{\text{var}}$  and that the coherent QP near  $(\pi, 0)$  must then reside at  $E_{\text{gap}}$  in order to be stable against decay into incoherent excitations. It is then plausible that  $\Delta_{\text{var}}$ , the large gap before projection, is related to an incoherent feature in  $A(\mathbf{k}, \omega)$  near  $(\pi, 0)$  after projection [15]. Indeed, comparing  $\Delta_{\text{var}}$  with the  $(\pi, 0)$  “hump” feature seen in ARPES [9], we find good agreement in the magnitude as well as doping dependence; see Fig. 1(a).

**Optical spectral weight:** The optical conductivity sum rule states that  $\int_0^\infty d\omega \text{Re}\sigma(\omega) = e^2\pi \sum_{\mathbf{k}} m^{-1}(\mathbf{k})n(\mathbf{k}) \equiv \pi D_{\text{tot}}e^2/2$  where  $m^{-1}(\mathbf{k}) = (\partial^2\epsilon(\mathbf{k})/\partial\mathbf{k}_x\partial\mathbf{k}_x)$  is the *noninteracting* mass tensor. The *total* optical spectral weight  $D_{\text{tot}}(x)$  is plotted in Fig. 5(a) and seen to be non-zero even at  $x = 0$ , since the infinite cutoff in the integral above includes contributions from the “upper Hubbard band”.

A physically more interesting quantity is the *low frequency* optical weight, or Drude weight,  $D_{\text{low}}$  where the upper cutoff extends above the scale of  $t$  and  $J$ , but is much smaller than  $U$ . This is conveniently defined [7] by the response to an external vector potential:  $D_{\text{low}} = \partial^2\langle\mathcal{H}_A\rangle_A/\partial A^2$ . Here the subscript on  $\mathcal{H}$  denotes that  $A$  enters the kinetic energy via a Peierls minimal coupling, and that on the expectation value denotes the corresponding modification of  $\exp(iS)$  in Eq. (1). The Drude weight  $D_{\text{low}}(x)$ , plotted in Fig. 5(a), vanishes linearly as  $x \rightarrow 0$ , which can be argued to be a general property of projected states [7]. This also proves, following Ref. [16], that  $|\Psi_0\rangle$  describes an insulator at  $x = 0$ . Both the magnitude and doping dependence of  $D_{\text{low}}(x)$  are consistent with optical data on the cuprates [17].

Motivated by our results on the nodal  $Z(x)$  and  $D_{\text{low}}(x)$ , we make a parametric plot of these two quantities in Fig. 5(b) and find that  $D_{\text{low}} \sim Z$  over the entire doping range, a prediction which can be checked by comparing optics and ARPES on the cuprates.

**Superfluid Density:** The Kubo formula for the superfluid stiffness can be written as  $D_s = D_{\text{low}} - \Lambda^T$ , where  $D_{\text{low}}$  is the diamagnetic response and  $\Lambda^T$  is the transverse current correlator. Using its spectral representation one can argue that  $\Lambda^T \sim x^2$  for small  $x$  [18]. Thus one finds that  $D_s \simeq D_{\text{low}} \sim x$  for  $x \ll 1$  as observed experimentally [19].

If one *assumes* that  $\Lambda^T \sim x^2$  over the *entire* range  $0 < x < x_c \simeq 0.35$ , then  $D_s(x) = D_{\text{low}}(x) - Cx^2$  where  $C$  can be determined by demanding that  $D_s(x_c) = 0$ . The resulting non-monotonic [19] superfluid density is plotted in Fig. 5(a). We find  $D_s \approx 50\text{meV}$  at optimality, implying a penetration depth  $\lambda \approx 1800\text{\AA}$ , in rough agreement with BSCCO [20].

**Implications for  $T \neq 0$  phase diagram:** We have shown within our variational scheme the  $T = 0$  evolution of the system from an undoped insulator to a d-wave SC to a Fermi liquid as a function of  $x$ . The SC order parameter  $\Phi(x)$  and superfluid stiffness  $D_s(x)$  are non-monotonic with a maximum at optimal doping  $x \simeq 0.2$ ,

suggestive of the experimental trend in  $T_c(x)$  from under- to over-doping. For  $x \ll 1$ ,  $D_s \sim x$  while the spectral gap, expected to scale with  $\Delta_{\text{var}}$ , remains finite. Thus the underdoped state, with strong pairing and weak phase coherence, should lead to pseudogap behavior in the temperature range between  $T_c$ , which scales like  $\Phi$ , and  $T^*$ , which scales like  $\Delta_{\text{var}}$ .

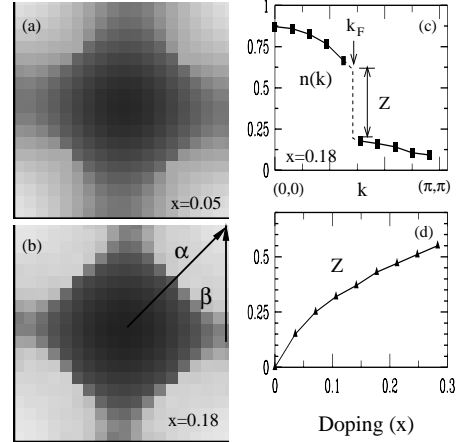


FIG. 2. (a) and (b): Gray-scale plots of  $n(\mathbf{k})$  (black  $\equiv 1$ , white  $\equiv 0$ ) centered at  $\mathbf{k} = (0, 0)$  for  $x = 0.05$  and  $x = 0.18$  respectively on a  $19 \times 19 + 1$  lattice, showing very little doping dependence of the large “Fermi surface”. (c):  $n(\mathbf{k})$  plotted along the diagonal direction (indicated as  $\alpha$  in Panel (b)), showing the jump at  $k_F$  which implies a gapless nodal quasiparticle of weight  $Z$ . (d): Doping dependence of the nodal quasiparticle weight, with  $Z \sim x$  for  $x \rightarrow 0$ .

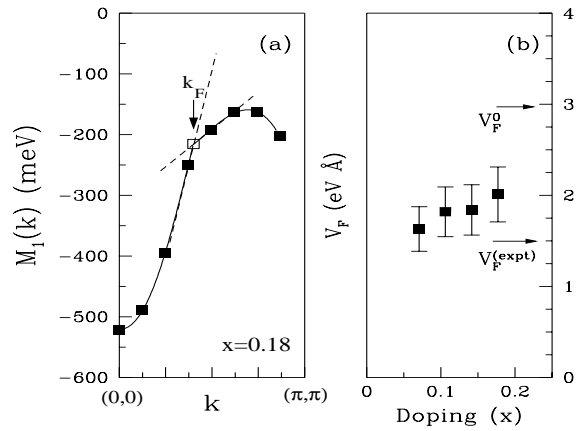


FIG. 3. (a): The moment  $M_1(\mathbf{k}) = \int d\omega \omega f(\omega) A(\mathbf{k}, \omega)$ , plotted along the zone diagonal, with smooth fits for  $k < k_F$  and  $k > k_F$ , showing discontinuity of  $Zv_F$  in the slope  $dM_1/dk(\mathbf{k} = k_F)$ . (b): Doping dependence of the nodal quasiparticle velocity obtained from  $M_1(\mathbf{k})$ . The 15% error bars are associated with the fits to  $M_1(\mathbf{k})$ . Also shown are the bare nodal velocity  $v_F^0$ , and the ARPES estimate  $v_F^{(\text{expt})}$  [12].

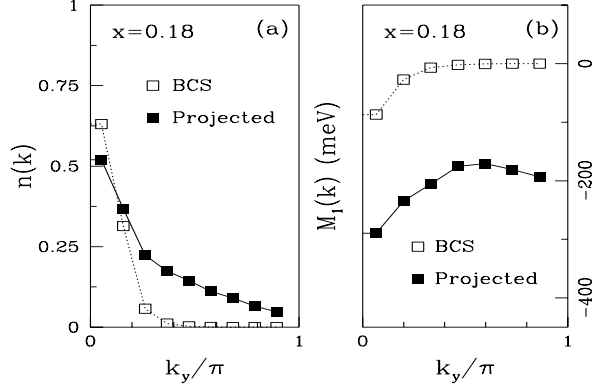


FIG. 4. (a):  $n(\mathbf{k})$  plotted along the  $(\pi, 0)$ - $(\pi, \pi)$  direction (indicated as  $\beta$  in Fig. 2(b)) and compared with the BCS result. (b): The moment  $M_1(\mathbf{k})$  plotted along the  $(\pi, 0)$ - $(\pi, \pi)$  direction compared with the BCS values.

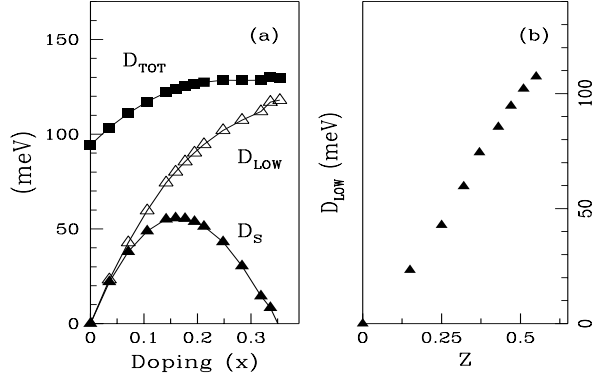


FIG. 5. (a): Doping dependence of the total ( $D_{\text{tot}}$ ) and low energy ( $D_{\text{low}}$ ) optical spectral weights and the superfluid stiffness  $D_s$ . (b): The optical spectral weight  $D_{\text{low}}$  versus the nodal quasiparticle weight  $Z$ .

**Acknowledgements:** M. R. was supported in part by the D. S. T. through the Swarnajayanti scheme.

[1] P. W. Anderson, Science **235**, 1196 (1987); G. Baskaran, Z. Zou and P. W. Anderson, Sol. St. Comm. **63**, 973 (1987); G. Kotliar and J. Liu, Phys. Rev. B **38**, 5142 (1988).  
[2] X. G. Wen and P. A. Lee, Phys. Rev. Lett. **78**, 4111 (1997); D. H. Lee, Phys. Rev. Lett. **84**, 2694 (2000).  
[3] (a) C. Gros, R. Joynt and T.M. Rice, Z. Phys. B **68**, 425 (1987); (b) C. Gros, Phys. Rev. **38**, 931 (1988); (c) E.S. Heeb and T.M. Rice, Europhys. Lett., **27**, 673 (1994).

[4] H. Yokoyama and H. Shiba, J. Phys. Soc. Jpn. **57**, 2482 (1988); H. Yokoyama and M. Ogata, J. Phys. Soc. Jpn. **65**, 3615 (1996).  
[5]  $\exp(-iS)\mathcal{H}\exp(iS)$  is often used to generate an effective tJ Hamiltonian. See: C. Gros, R. Joynt and T.M. Rice, Phys. Rev. B, **36**, 381 (1987); A. H. Macdonald, S. M. Girvin and D. Yoshioka, Phys. Rev. B **37**, 9753 (1988). We find it more convenient to include the  $\exp(iS)$  factor in the wavefunction instead.  
[6] Since the pair wavefunction  $\varphi(\mathbf{k})$  is singular on the zone diagonal we use “tilted” lattices [3] with periodic boundary conditions. Most results were obtained on a  $15 \times 15 + 1$  site lattice, with some on a  $19 \times 19 + 1$  lattice to reduce finite size effects for the order parameter (at overdoping) and improve  $\mathbf{k}$ -resolution for  $n(\mathbf{k})$ . Typically we used 5000 equilibration sweeps, and averaged over 500-1000 configurations from 5000 sweeps.  
[7] Details will be presented in a longer paper; A. Paramekanti, M. Randeria and N. Trivedi (unpublished).  
[8] To put a pair of electrons on a link near  $\mathbf{r}$ , after removing them from a link near the origin, requires two vacancies near  $\mathbf{r}$ . Thus  $F_{\alpha,\alpha}(\mathbf{r}) \sim x^2$  and  $\Phi \sim x$  as  $x \rightarrow 0$ .  
[9] J. C. Campuzano *et al.*, Phys. Rev. Lett. **83**, 3709 (1999).  
[10] H. Ding *et al.*, Phys. Rev. Lett. **78**, 2628 (1997); F. Ronning *et al.*, Science **282**, 2067 (1998).  
[11] The Fourier transform of  $M_1(\mathbf{k})$  is  $M_1(\mathbf{r} - \mathbf{r}') = -t_{\mathbf{r}\mathbf{r}'} \langle c_{\sigma}^{\dagger}(\mathbf{r})c_{\sigma}(\mathbf{r}') \rangle + U \langle c_{\sigma}^{\dagger}(\mathbf{r})c_{\sigma}(\mathbf{r}')n_{\overline{\sigma}}(\mathbf{r}') \rangle$ . Since the second term is  $\mathcal{O}(U)$  we need  $S$  in Eq. (1) to  $\mathcal{O}(t/U)^2$  to obtain  $M_1(\mathbf{k})$  correctly to  $\mathcal{O}(J)$ .  
[12] A. Kaminski *et al.*, Phys. Rev. Lett. **84**, 1788 (2000); and cond-mat/0004482, Phys. Rev. Lett. (to appear).  
[13] Relating  $Z$  to the amplitude of the asymptotic power-law decay in  $\langle c_{\sigma}^{\dagger}(\mathbf{r})c_{\sigma}(\mathbf{r}') \rangle$  we can show that  $Z \sim x$  for projected states [7].  
[14] For unprojected BCS wavefunctions we can estimate  $v_F$  with 5% accuracy using this method on finite systems.  
[15] We find numerically that  $|M_1(\pi, 0) - M_1(k_F^{\text{node}})| \sim \Delta_{\text{var}}$  for all  $x$ .  
[16] A. J. Millis and S. N. Coppersmith, Phys. Rev. B **42**, 10807 (1990) and Phys. Rev. B **43**, 13770 (1991).  
[17] Using a lattice spacing  $a = 3.85\text{\AA}$  for BSCCO we find  $(\omega_p^*)^2 \equiv (4\pi e^2/a)D_{\text{low}} \approx (1.8\text{eV})^2$  at optimal doping, in good agreement with data summarized in S. L. Cooper *et al.*, Phys. Rev. B **47**, 8233 (1993).  
[18] For  $x \rightarrow 0$ , the current operator matrix elements  $\langle n|J(\mathbf{q} \rightarrow 0)|0 \rangle \sim x$ , while the excitations contributing to  $\Lambda^T$  are not expected to depend strongly on  $x$ .  
[19] Y. J. Uemura *et al.*, Phys. Rev. Lett. **62**, 2317 (1989); Ch. Niedermayer *et al.*, Phys. Rev. Lett. **71**, 1764 (1993).  
[20] The agreement with the measured  $\lambda \simeq 2100\text{\AA}$  [S. F. Lee *et al.*, Phys. Rev. Lett. **77**, 735 (1996)] would be improved by including the effects of long wavelength quantum phase fluctuations; see A. Paramekanti *et al.*, Phys. Rev. B **62**, 6786 (2000), L. Benfatto *et al.*, cond-mat/0008100.